

# Synthesis and Structural Characterization of Sandwich-Type Keggin- $\gamma$ -Lacunary Silicotungstates with an Open Wells–Dawson-Like Structure

Hongsheng Liu,<sup>[a]</sup> Jun Peng,<sup>\*[a]</sup> Zhongnin Su,<sup>[a]</sup> Yanhui Chen,<sup>[a]</sup> Baoxia Dong,<sup>[a]</sup>  
Aixiang Tian,<sup>[a]</sup> Zhangang Han,<sup>[a]</sup> and Enbo Wang<sup>[a]</sup>

**Keywords:** Polyoxometalates / Tungstosilicates / Keggin structures / Transition metals

Three novel  $[\gamma\text{-SiW}_{10}\text{O}_{36}]^{8-}$  dimers,  $[\{\text{K}(\text{H}_2\text{O})\}_2(\mu_3\text{-H}_2\text{O})\text{M}(\text{H}_2\text{O})\{\gamma\text{-Si}_2\text{W}_{20}\text{O}_{70}\}]^{8-}$  ( $\text{M} = \text{Mn}^{2+}$ , **1**;  $\text{Co}^{2+}$ , **2**;  $\text{Ni}^{2+}$ , **3**), are isolated from an aqueous acidic medium without isomerization, which is different from most reactions of  $[\gamma\text{-SiW}_{10}\text{O}_{36}]^{8-}$  with first-row transition metals. They are isomorphous and crystallize in the orthorhombic system, space group  $Pnma$ .

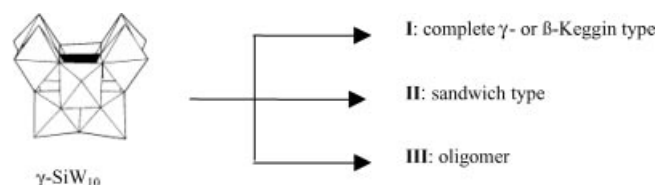
These species are the first examples of imidazole–potassium mixed salts of Keggin- $\gamma$ -type dimers having an analogous open structure related to the Wells–Dawson anionic cluster.

(© Wiley-VCH Verlag GmbH & Co. KGaA, 69451 Weinheim, Germany, 2006)

## Introduction

Polyoxometalates (POMs), a well-known, large, and unique class of inorganic polynuclear compounds, are the focus of numerous interdisciplinary projects in recent years owing to their special redox properties and tunable structure variety. This research area, as summarized in a vivid meeting review by Kögler and Cronin, has undergone “an important transition from classical inorganic chemistry towards the chemistry of “smart”, “functional materials”.”<sup>[1]</sup> Among thousands of POM compounds, the metastable lacunary polyoxotungstates, such as Keggin-type 9-series  $[\text{AW}_9\text{O}_{34}]^{7-}$  ( $\text{A} = \text{P}, \text{Si}, \dots$ ), 10-series  $[\gamma\text{-AW}_{10}\text{O}_{36}]^{8-}$ , 11-series  $[\text{AW}_{11}\text{O}_{39}]^{8-}$ , and Wells–Dawson-type  $[\text{P}_2\text{W}_{15}\text{O}_{56}]^{12-}$ ,  $[\text{P}_2\text{W}_{17}\text{O}_{61}]^{10-}$ , and so on, bearing an analogy with porphyrin, have drawn increasing attention as structural fragments or building blocks due to their versatility to generate unexpected species with surprising structures and multiple properties, which include catalytic, medicinal, magnetic, electronic, and optical properties.<sup>[2]</sup> Especially, mono- and trivacant  $\alpha$ - and  $\beta$ -Keggin polyoxoanions have been studied for many years and are in general understood.<sup>[3]</sup> On the contrary, investigation of the divacant  $\gamma$ -Keggin polyoxoanion  $[\gamma\text{-SiW}_{10}\text{O}_{36}]^{8-}$  ( $\gamma\text{-SiW}_{10}$ ), first reported by Hervé et al.,<sup>[4]</sup> is less perhaps due to its poor stability in aqueous solution. However, extensive studies on  $\gamma\text{-SiW}_{10}$  are prompted by very interesting results that have been reported in recent years,<sup>[5–20]</sup> from which three kinds of derivatives, **I**, **II**, and **III** symbolized in Scheme 1, can be summarized.

Derivative **I** represents the derivatives in which the  $\gamma\text{-SiW}_{10}$  anion accommodates the two vacant positions to two transition-metal atoms or other groups to generate the complete or modified  $\gamma$ - or  $\beta$ -Keggin anions; derivative **II** represents the sandwich-type derivatives in which two  $\gamma\text{-SiW}_{10}$  subunits associate together by additional bridges; derivative **III** represents oligomeric derivatives in which the  $\gamma\text{-SiW}_{10}$  anions are isomerized and polymerized by transition metal ions.



Scheme 1. Three kinds of derivatives synthesized from the precursor  $[\gamma\text{-SiW}_{10}\text{O}_{36}]^{8-}$  anion.

Kortz and co-workers carried out a systematical study on the reaction of  $\gamma\text{-SiW}_{10}$  anions with first-row transition metals from which they isolated a series of isomerized oligomers ranging in size from dimers to tetramers. They found that the dilacunary precursor isomerized easily in an aqueous acidic medium upon heating and in the presence of first-row transition metal ions, unlike the 9-series and 2:18-series whose structures could be preserved in the sandwich-type products. Accordingly, sandwich-type  $\gamma\text{-SiW}_{10}$  dimers are still a challenge to obtain for POM chemists. Up to now, only Pope's group has reported a sandwich-type  $\gamma\text{-SiW}_{10}$  dimer that was isolated as a cesium salt.<sup>[13]</sup> In our efforts to modify POM clusters,<sup>[21]</sup> we obtained three novel compounds with the  $[\gamma\text{-SiW}_{10}\text{O}_{36}]^{8-}$  fragment preserved. Herein we report the syntheses and structural characterization of them. They possess an open Wells–Dawson-like

[a] Key Laboratory of Polyoxometalate Science of Ministry of Education, Faculty of Chemistry, Northeast Normal University, Changchun 130024, P. R. China  
E-mail: jpeng@nenu.edu.cn

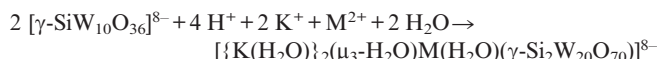
Supporting information for this article is available on the WWW under <http://www.eurjic.org> or from the author.

structure in which two  $\gamma$ -SiW<sub>10</sub> subunits are directly associated to each other in an eclipsed fashion. To the best of our knowledge, this type of structure that is constructed from  $\gamma$ -SiW<sub>10</sub> has not yet been reported until now. From a structure point of view, only  $[\alpha\text{-Si}_2\text{W}_{18}\text{O}_{66}]^{22-}$  was an analog.

## Results and Discussion

### Synthesis

The title compounds were isolated from an acidic solution containing  $\gamma$ -SiW<sub>10</sub>, transition-metal cations, and imidazole under gentle conditions, illustrated by the reaction:



It deserves to be mentioned that the  $\gamma$ -silicodecatungstate is a metastable species and easily isomerizes to  $\alpha$ - or  $\beta$ -species, such as  $\alpha$ -dodecasilicotungstates and  $\beta$ -undecasilicotungstates.<sup>[18]</sup> Therefore, a key problem is to inhibit its decomposition and isomerization during the reaction process in order to keep the anionic skeleton intact. Slight changes in the reaction conditions, such as temperature or pH, may influence the final products. The synthetic conditions of the compounds reported from precursor  $\text{K}_8[\gamma\text{-SiW}_{10}\text{O}_{36}]$  are collected in Table 3. From Table 3 it can be found that lower or higher pH values ( $3 > \text{pH} > 5$ ), elevated temperatures ( $\geq 50^\circ\text{C}$ ), and long reaction times ( $\geq 30$  min) are favorable for the decomposition and reassembly or isomerization of  $\gamma$ -SiW<sub>10</sub>, whereas the presence of an organic solvent or bigger cations such as  $\text{K}^+$ ,  $\text{Rb}^+$ , and  $\text{Cs}^+$  would increase the stability of the  $\gamma$ -SiW<sub>10</sub> skeleton.<sup>[25–27]</sup> In the preparation process we controlled the reaction temperature to a maximum of  $45^\circ\text{C}$  and the pH wave to not more than  $\pm 0.3$ . It is worthy to mention that imidazole–potassium mixed salts are obtained but only two  $\text{K}^+$  ions are included in the crystal structures of the compounds even though excessive amounts of  $\text{K}^+$  ions are present in the reaction solution.

The role of the  $\text{K}^+$  ion in the reaction is conjectured as illustrated in Scheme 2: two  $\text{K}^+$  ions occupy the pseudosymmetrical position in front of the aperture of the structure.<sup>[4]</sup> Because of the strong coordinative tendency of  $\text{K}^+$  to bind to the open facial oxygen atoms,<sup>[22]</sup> two  $\gamma$ -SiW<sub>10</sub> subunits combine through them. The insertion of transition metal ions and the interjunction of two  $\gamma$ -SiW<sub>10</sub> subunits would enhance the coordination of  $\text{K}^+$  to the surrounding oxo ligands, which would lead to stability of the open Wells–Dawson-like structure.

Additionally, the simulative and experimental powder X-ray diffraction patterns of **1** and **2** are coincident as well, which confirms that the as-prepared compounds are pure (see Figure S3).

### Structure Description

Compounds **1**, **2**, and **3** are isomorphic and are isolated as imidazole salts of the  $\gamma$ -SiW<sub>10</sub> derivative. The anion is a dimer of  $[\gamma\text{-SiW}_{10}\text{O}_{36}]^{8-}$  subunits that are jointed together by two adjacent terminal oxygen atoms Od' (Od', initially marked by Hervé<sup>[4]</sup> corner-shared with two pairs of edge-shared WO<sub>6</sub> octahedra from two parent  $[\gamma\text{-SiW}_{10}\text{O}_{36}]^{8-}$  anions (see Figure 1 and Figure S1).

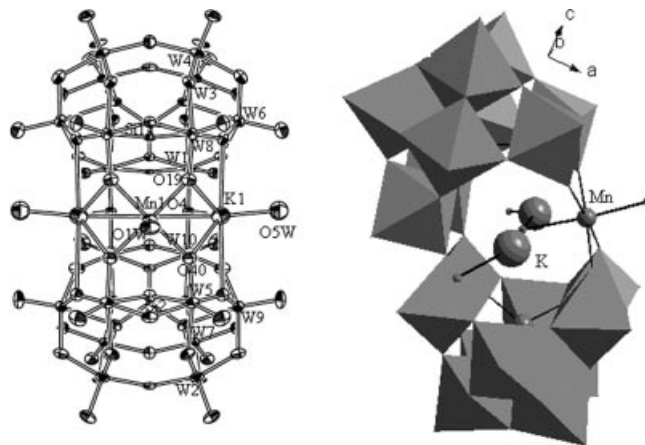
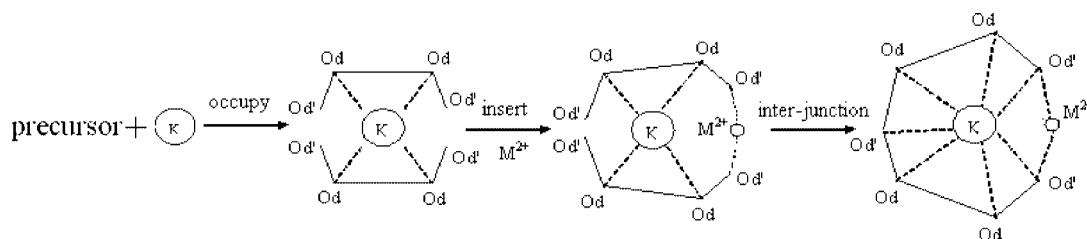


Figure 1. Structure of anion in **1**: the ORTEP view showing the atom-labeling scheme with 50% thermal ellipsoids (left); combined polyhedral/ball and stick representation (right), tungsten–oxygen octahedra, Si (big ball), oxygen (small ball), potassium (labeled), manganese (labeled). All hydrogen atoms are omitted for clarity.

In **1**, eight open facial bridging Ob atoms (four in each  $\gamma$ -SiW<sub>10</sub> subunit), two oxygen atoms of the W–Od'–W junctions (shared between two  $\gamma$ -SiW<sub>10</sub> subunits) and the remaining four Od' atoms (two in each  $\gamma$ -SiW<sub>10</sub> subunit), totaling fourteen oxygen atoms, delimit the open “mouth”. The four Od' atoms of the edge-shared WO<sub>6</sub> octahedral dimer in the hatch of the  $[\gamma\text{-Si}_2\text{W}_{20}\text{O}_{70}]$  cluster are strongly basic to form active sites, either for protonation or for coordination,<sup>[23]</sup> which is a characteristic reminiscent of porphyrin. One  $\text{Mn}^{\text{II}}$  ion is coordinated by the four Od' atoms like sharp incisors biting a  $\text{Mn}^{\text{II}}$  ion. Perpendicular to the plane of the  $\text{MnOd}'_4$ , two  $\text{H}_2\text{O}$  molecules coordinate to the  $\text{Mn}^{\text{II}}$  center to complete an octahedral coordination environment.



Scheme 2. Illustration of possible role of  $\text{K}^+$  ions in the formation of the open Wells–Dawson-like structure.

of Mn<sup>II</sup>, one towards the outside (O2W) and the other towards the inside (O1W). Interestingly, the “internal” H<sub>2</sub>O, acting as a tri-bridge H<sub>2</sub>O ( $\mu_3$ -H<sub>2</sub>O), links two K<sup>+</sup> ions in the middle point of the K<sup>+</sup>-to-K<sup>+</sup> line; thus, a T-type connection composed of K<sup>+</sup>,  $\mu_3$ -H<sub>2</sub>O and Mn<sup>II</sup> is formed (see Figure 2a). In fact, two K<sup>+</sup> ions are located separately on the two parotids of the “mouth”, each bonding to seven oxygen atoms; thus, a nine-coordination sphere of the K<sup>+</sup> ion is accomplished by the coordination of the inside  $\mu_3$ -H<sub>2</sub>O and the outside H<sub>2</sub>O molecules (see Figure 2b). The K–OW bond lengths are in the range 2.80(6)–2.84(2) Å, and seven K–O bond lengths [2.96(1)–3.13(1) Å] correspond to the range (2.76–3.22 Å) reported by Hervé.<sup>22</sup> The W1–O4–W10 angle of the junctions is 135.1° and the bond lengths are 1.85(1) Å and 2.02(1) Å, respectively, which is in the normal range for corner W–O–W bridges in each subunit (See Figure S2 for the coordination spheres of **2** and **3**).

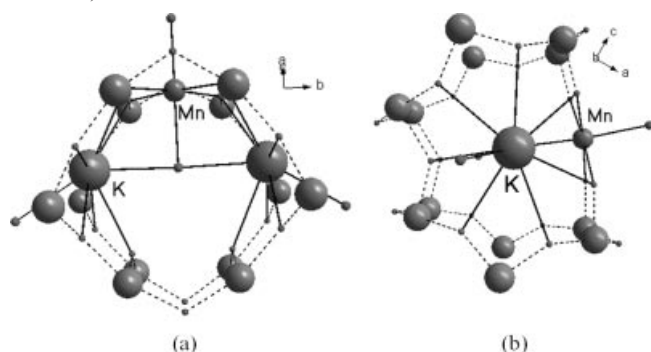


Figure 2. Coordination spheres of K<sup>+</sup> and Mn<sup>2+</sup> in compound **1**: (a) viewed along the normal direction of the  $\nabla$  K–M–K plane, (b) viewed along the line of K–OW<sub>int</sub>–K, tungsten (big ball), oxygen (small ball), potassium (labeled), manganese (labeled).

It is interesting to make a comparison with the filling manners of the “mouths” for the [ $\gamma$ -Si<sub>2</sub>W<sub>20</sub>O<sub>70</sub>] and [ $\alpha$ -Si<sub>2</sub>W<sub>18</sub>O<sub>66</sub>] clusters. The “mouth” of [ $\alpha$ -Si<sub>2</sub>W<sub>18</sub>O<sub>66</sub>] seems

to be more open than that of [ $\gamma$ -Si<sub>2</sub>W<sub>20</sub>O<sub>70</sub>]. In the former, there exist several filling manners of the “mouth” or “pocket”, such as K<sub>3</sub>, KCo, and KCo<sub>2</sub>, whereas in the latter the filling manners seem to be more regular, as only K<sub>2</sub>M (M = Mn<sup>II</sup>, Co<sup>II</sup>, or Ni<sup>II</sup>) is found.

Selected bond lengths and angles of compounds **1**, **2**, and **3** are listed in Table 1 along with those of the [ $\gamma$ -SiW<sub>10</sub>O<sub>36</sub>]<sup>8-</sup> precursor for comparison. From Table 1 we can see that the bond lengths of Si–Oa (W<sub>2</sub> diad) (the oxygen atom belongs to a ditungstic group) are longer in compounds **1**, **2**, and **3** than those of the [ $\gamma$ -SiW<sub>10</sub>O<sub>36</sub>]<sup>8-</sup> precursor, whereas those of Si–Oa (W<sub>3</sub> triad) (the oxygen atom belongs to a tritungstic group) are shorter, that is, the Si–Oa bond lengths go to an average value that is close to 1.63 Å for [ $\alpha$ -SiW<sub>12</sub>O<sub>40</sub>]<sup>4-</sup>.<sup>[1]</sup> This would enhance the stability of **1**. Other W–O bond lengths are within their normal values, except for the longer W10–Od (O31) and W10/W1–Od' (O4) bonds which are the junctions of the two SiW<sub>10</sub> subunits (see Table S1). The corresponding bond lengths and bond angles of the transition metal in the hatches of [ $\gamma$ -Si<sub>2</sub>W<sub>20</sub>O<sub>70</sub>] for **1**, **2**, and **3** are listed in Table 2 along with those of [ $\alpha$ -Si<sub>2</sub>W<sub>18</sub>O<sub>66</sub>] for comparison. The average bond lengths of M–Od' are 2.12 Å for **1**, 2.05 Å for **2**, and 2.03 Å for **3**, and the W–O–W bond angles of the junctions are smaller than that of [ $\alpha$ -Si<sub>2</sub>W<sub>18</sub>O<sub>66</sub>].

The anion packing diagram in the unit cell of **1** viewed down the *b* axis is given in Figure 3a. There are four anions labeled as A, A\*, B, and B\*. The two adjacent anions A and A\* or B and B\* are, respectively, related by an inversion center and associated with each other in a “mouth-to-mouth” manner by imidazole molecules with the Mn<sup>II</sup>–Mn distance of 8.37 Å. Anions A\* and B arrange in a “head-to-head” manner on the same plane, and B\* and A run in this manner on another plane (Figure 3b). Thus A\*...B...A\*...B and B\*...A...B\*...A form zigzag chains along the *a* axis, respectively, and further extend into a 2D structure along the *c* axis by hydrogen bonding with Im

Table 1. Selected bond length ranges [Å] for **1**, **2**, and **3**.

Bond length	[ $\{K(H_2O)_2\}_2\{\mu_3(H_2O)M(H_2O)\}(\gamma\text{-Si}_2W_{20}O_{70})\}^{8-}$ ]			[ $\gamma$ -SiW <sub>10</sub> O <sub>36</sub> ] <sup>8–[4]</sup>
	<b>1</b> (M = Mn <sup>II</sup> )	<b>2</b> (M = Co <sup>II</sup> )	<b>3</b> (M = Ni <sup>II</sup> )	
W–Oa	2.22(1)–2.36(1)	2.21(10)–2.36(1)	2.21(1)–2.35(1)	2.21(5)–2.34(4)
W–Ob/Oc	1.76(1)–2.16(1)	1.78(1)–2.14(1)	1.78(1)–2.14(1)	1.73(5)–2.25(5)
W–Od	1.71(1)–1.88(2)	1.71(1)–1.88(1)	1.70(1)–1.84(1)	1.67(5)–1.77(4)
W–Od'	1.76(1)–2.02(1)	1.78(1)–1.98(1)	1.78(1)–1.96(1)	1.70(5)–1.79(4)
Si–Oa (W <sub>2</sub> diad)	1.62(1)–1.63(1)	1.59(1)–1.62(1)	1.60(1)–1.64(1)	1.54(5)–1.59(5)
Si–Oa (W <sub>3</sub> triad)	1.65(1)–1.65(1)	1.64(1)–1.65(1)	1.64(1)–1.64(1)	1.68(4)–1.68(4)

Table 2. Comparison of the corresponding bond length [Å] and bond angle [°] of metal polyhedrons.

Bond length/angle	[ $\gamma$ -Si <sub>2</sub> W <sub>20</sub> O <sub>70</sub> ] in <b>1–3</b>			[ $\alpha$ -Si <sub>2</sub> W <sub>18</sub> O <sub>66</sub> ] <sup>[22]</sup> 1Co–K
	<b>1</b> (M = Mn <sup>II</sup> )	<b>2</b> (M = Co <sup>II</sup> )	<b>3</b> (M = Ni <sup>II</sup> )	
K–O	2.97(1)–3.13(1)	2.94(1)–3.09(1)	2.93(1)–3.08(1)	2.76–3.22
K–OW(inside)	2.80(6)	2.75(9)	2.77(1)	
K–OW(outside)	2.84(2)	2.59(5)–2.67(4)	2.58(6)–2.61(7)	2.669–3.162 (for K9 and K11)
M–OW(inside)	2.43(1)	2.22(1)	2.192(1)	
M–OW(outside)	2.29(2)	2.09(2)	2.04(1)	
M–Od'	2.12(1)–2.12(1)	2.04(1)–2.05(1)	2.02(1)–2.03(1)	
W–O–W junction	135.1(6)	136.4(6)	136.6(7)	147.7–148.2

Table 3. Comparison of the synthetic conditions from precursor  $K_8[\gamma\text{-SiW}_{10}\text{O}_{36}]$ .

Compound <sup>[a]</sup>	pH	<i>T</i> [°C]	<i>t</i>	Ref.
<b>I</b> a) $[(C_4H_9)_4N]_4[(SiO_4)W_{10}Mn^{III}_2O_{36}H_6]$	3.8–4.5	–	5 min	[5]
<b>I</b> b) $Cs_5[\gamma\text{-SiO}_4W_{10}O_{32}(OH)Cr_2(OOCCH_3)_2(OH_2)_2]$	4.8	80	30 min	[6]
<b>I</b> c) $[(n\text{-C}_4\text{H}_9)_4N]_{3.5}H_{2.5}[\gamma\text{-SiW}_{10}\{Fe(OH_2)\}_2O_{38}]$	3.9	–	5 min	[7]
<b>I</b> d) $Cs_4H_2\text{-}\gamma(1,2)\text{-}[SiV_2W_{10}O_{40}]$	–	–	few min	
<b>I</b> d) $Cs_6\text{-}\beta(8,12)\text{-}[SiV_2W_{10}O_{40}]$	6.5–6.8	–	4 h	[8]
<b>I</b> d) $Cs_6\text{-}\beta(3,8)\text{-}[SiV_2W_{10}O_{40}]$	8.0–8.3	–	10 min	
<b>I</b> e) $(Bu_4N)_3H[\gamma\text{-SiW}_{10}O_{36}(RSi)_2O]$	$CH_3CN/HCl$	–	6 h	[9]
<b>I</b> f) $(NEt_4)_6[\gamma\text{-SiW}_{10}Mo_2S_2O_{38}]$	DMF	50	30 min	[10]
<b>I</b> g) $(NBu_4)_3K[\gamma\text{-SiW}_{10}O_{36}(HPO)_2]$	$CH_3CN/HCl$	–	overnight	[11]
<b>I</b> h) $[(CH_3)_2NH_2]_5[\beta\text{-SiFe}_2W_{10}O_{36}(OH)_2(H_2O)Cl]$	1.7	–	5 min	[12]
<b>II</b> a) $Cs_9H[(PhSnOH)_2(\gamma\text{-SiW}_{10}O_{36})_2]$	–	–	rapid	[13a]
<b>II</b> b) $K_xNa_{12-x}[\{\{SiM_2W_9O_{34}(H_2O)\}_2\}^{12-}(M = Mn^{2+}, Cu^{2+}, Zn^{2+})]$	4.8	90	40 min	[14]
<b>III</b> a) $K_{12}[\{\beta\text{-SiNi}_2W_{10}O_{36}(OH)_2(H_2O)\}_2]$	4.8	50	45 min	[15]
<b>III</b> b) $K_{24}[\{\beta\text{-Ti}_2SiW_{10}O_{39}\}_4]$	2	80	1 h	[16]
<b>III</b> c) $Na_5[Co_6(H_2O)_{30}\{Co_9Cl_2(OH)_3(H_2O)_9(\beta\text{-SiW}_8O_{31})_3\}]$	5.5	50	30 min	[17]
<b>III</b> d) $Cs_4K_{11}[(\beta_2\text{-SiW}_{11}MnO_{38}OH)_3]$	3.9	–	15 min	[18]
<b>III</b> e) $K_{10}Na_{12}[\{Co_3(\beta\text{-}\beta\text{-SiW}_9O_{33}(OH))(\beta\text{-}\beta\text{-SiW}_8O_{29}(OH)_2)_2\}]$	4.8	50	30 min	[19]
<b>III</b> f) $Rb_6H_3[Si_2W_{23}O_{77}(OH)]$	$HClO_4$	–	1 h	[20]

[a] **I**: complete  $\gamma$ - or  $\beta$ -Keggin-type **II**: sandwich-type **III**: oligomer.

molecules. There are significant contacts between oxo groups of the anions and imidazole molecules along the *b* axis, which leads to a linear chain of the anions with a straight linkage of  $K\cdots K\cdots K$  (see Figure 4). Imidazole and water molecules fill in the space among the anions.

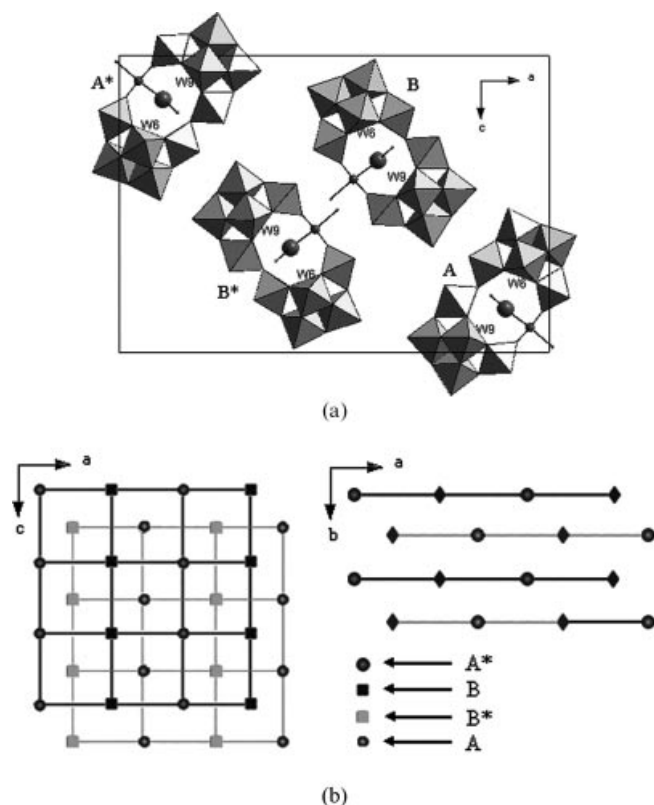


Figure 3. Schematic representation of the relative locations of the polyanions. (a) Packing diagram in **1** viewed along the *b* axis. (b) 3D supramolecular network based on the topology of anion-anion position.

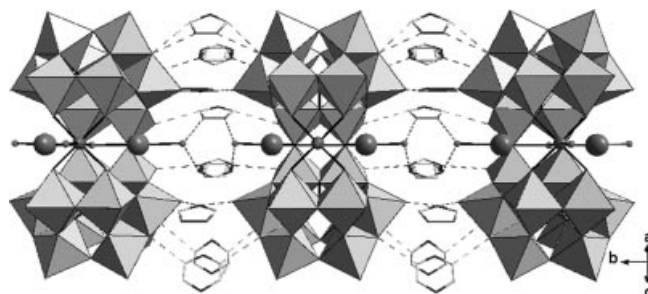


Figure 4. View of the connection between the polyanions and Im molecules through hydrogen bonding. All water molecules are omitted for clarity.

Because compounds **2** and **3** are isomorphs of **1**, structural descriptions for them are omitted. The difference between them is that the outer  $H_2O$  molecule that is coordinated to the  $K^+$  ion is disordered with an occupancy factor of 50% for both **2** and **3**. Additionally, there exists other disordered water and imidazole molecules in the crystal structures of these three complexes.

The assignment of the oxidation state of Mn is based on bond valence sum (BVS) calculations,<sup>[24]</sup> which gives a value of 2.064 and indicates the +2 oxidation state. The inside O atom and the outside O atom of the Mn–O bonds have much lower BVS values, 0.180 and 0.252, which suggests that they are water ligands (O1W and O2W). The BVS values of the bridge and terminal oxygen atoms show that they are not protonated. While in the acidic condition, the N atom of imidazole is easily protonated and leads to the formation of the stable salts. Thus, including  $K^+$  and  $M^{II}$ , the anionic structure can be written as  $[\{K(H_2O)\}_2\{\mu_3\text{-}H_2O\}M(H_2O)\{Si_2W_{20}O_{70}\}]^{8-}$  ( $M = Mn^{2+}, Co^{2+}$  or  $Ni^{2+}$ ). Overall, the anions have an ideal symmetry of  $C_{2v}$ .



## IR Spectra

The infrared spectra of **1**, **2**, and **3**, measured in the range 400–1000 cm<sup>-1</sup>, show characteristic absorptive peaks for the  $\gamma$ -anion at ca. 993 cm<sup>-1</sup> for  $\nu_{\text{as}}(\text{W–Od})$ , 940 cm<sup>-1</sup> for  $\nu_{\text{as}}(\text{Si–Oa})$ , 895 and 861 cm<sup>-1</sup> for  $\nu_{\text{as}}(\text{W–Ob–W})$ , 780 and 741 cm<sup>-1</sup> for  $\nu_{\text{as}}(\text{W–Oc–W})$ , which indicates the retention of the  $\gamma$ -tungstosilicate framework (see Figure S4).<sup>[6]</sup> In comparison with the  $\nu_{\text{as}}(\text{W–O–W})$  in  $\gamma$ -SiW<sub>10</sub>, the splitting of the corresponding bands in the range 700–850 cm<sup>-1</sup> is weakened in the title compounds and is due to the coordination of the transition metal ion, as in the case of the monosubstituted tungstosilicate. Additionally, the vibration bands in the range 1000–1200 cm<sup>-1</sup> are assigned to those of imidazole and around 620 cm<sup>-1</sup> to those of the M–O bonds.

## Thermogravimetric(TG) Analysis

The TG curve for **1** is divided into three stages. The first weight loss of 3.05% in the temperature range 45–180 °C corresponds to the release of crystal water and is in good agreement with the calculated value of 3.1%. The successive weight loss of the second step (5.68%) from 200 °C to 350 °C and the third step (7.93%) from 520 °C to 750 °C is ascribed to the release of imidazole and structural water, respectively, which is around the combined calculated value of 13.16%. No weight loss occurs above 750 °C. TG for **2** (see Figure S5) is similar to that of **1**.

## Cyclic Voltammetry (CV)

The CV behaviors of **1**, **2**, and **3** are similar (see Figure 5). Each CV curve shows two pairs of redox peaks with  $E_1 = -582$  mV and  $E_2 = -685$  mV for **1**,  $E_1 = -581$  mV and  $E_2 = -688$  mV for **2**, and  $E_1 = -570$  mV and  $E_2 = -675$  mV for **3**, where  $E = (E_{\text{pa}} + E_{\text{pc}})/2$ , in 0.5 M KAc/HAc buffer (pH 3.9). The anodic-to-cathodic peak potential difference

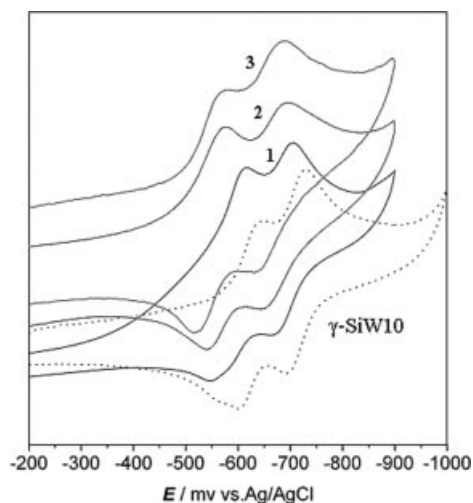


Figure 5. The cyclic voltammogram (glassy-carbon working electrode, scan-rate 50 mV s<sup>-1</sup>, 0.5 M KAc–HAc, pH = 3.9) of compounds **1**, **2**, and **3** and precursor  $\gamma$ -SiW<sub>10</sub>.

for each pair of redox waves is ca. 30 mV and the peak-to-peak distance between  $E_1$  and  $E_2$  is ca. 100 mV for each compound, which shows a similar electrochemical behavior to that of the parent  $\gamma$ -SiW<sub>10</sub>, except that the half-wave potentials shift positively. These can be reasonably explained by the global charges of the polyanions. Both of the anions, [ $\{\text{K}(\text{H}_2\text{O})\}_2(\mu_3\text{-H}_2\text{O})\text{M}(\text{H}_2\text{O})(\gamma\text{-Si}_2\text{W}_{20}\text{O}_{70})\}]^{8-}$  and [ $\gamma\text{-SiW}_{10}\text{O}_{36}\}]^{8-}$ , are in the -8 charge state, while the anion volume of the former is double that of the latter, which leads to less electronic density on the anion global.

## Conclusions

In summary, three novel compounds based on  $\gamma$ -SiW<sub>10</sub> subunits have been isolated in acidic solutions. They are successful examples of the  $\gamma$ -SiW<sub>10</sub> derivative possessing an open Wells–Dawson-like sandwich structure with K<sup>+</sup> and M<sup>II</sup> ions symmetrically enmeshed in the hatch of the ( $\gamma$ -SiW<sub>10</sub>)<sub>2</sub> dimer, giving the compound structural aesthetics. To check if the solid structure is stable in solution without the dissociation of the potassium cations, electrophoresis of compound **1** was carried out. The analytical result of the anodic area indicates that the potassium cations are attached to the polyoxo dimers and move towards the anode direction. This fact supports the polyanion structure formulated by [ $\{\text{K}(\text{H}_2\text{O})\}_2(\mu_3\text{-H}_2\text{O})\text{M}(\text{H}_2\text{O})(\gamma\text{-Si}_2\text{W}_{20}\text{O}_{70})\}]^{8-}$  and that the solid structure of the dimeric anions is maintained in the solution without the dissociation of the potassium cations, under the tested pH of 3.6.

This new crystal structure suggests that the skeleton of the unstable species  $\gamma$ -SiW<sub>10</sub> could also be maintained by carefully controlling the reaction conditions. The functions of potassium and transition-metal ions in the reactions of  $\gamma$ -SiW<sub>10</sub> are not clearly understood yet and attempts to clarify them still represent a challenge. Kortz and co-workers have emphasized the crucial role of potassium ions in the synthesis medium, especially in the order of addition of the solid KCl.<sup>[13]</sup> The title compounds were isolated under similar reaction conditions to those reported by Kortz and co-workers. However, they obtained full potassium salts and we obtained imidazole–potassium mixed salts of Keggin- $\gamma$ -type dimers. Besides the presence of imidazole, the difference in the order of addition of the solid KCl perhaps is the reason why mixed salts were crystallized in our case. Kortz's and our synthetic investigations both lead to the conclusion that the formation of the dimers is highly sensitive to pH and temperature variations.

The filling style in the “mouth” of the [ $\gamma$ -Si<sub>2</sub>W<sub>20</sub>O<sub>70</sub>] is perhaps less random than those of the [ $\alpha$ -Si<sub>2</sub>W<sub>18</sub>O<sub>66</sub>] because of the feature of the opening. The external H<sub>2</sub>O ligand that is coordinated to M<sup>II</sup> is likely to improve the catalytic activity and would be a further derivative of the polytungstates. We will attempt to modify the framework so as to obtain more unexpected species with interesting structure and properties.

## Experimental Section

**Materials and Methods:** The precursor  $K_8[\gamma\text{-SiW}_{10}\text{O}_{36}]\cdot 12\text{H}_2\text{O}$  was prepared according to the literature<sup>[28]</sup> and its purity was confirmed by infrared spectroscopy and cyclic voltammetry. All other reagents were used as purchased without further purification. Elemental analyses were carried out with a Plasma-Spec(I) ICP emission spectrometer for W, Si, and transition metal elements and with a PE-3030 atomic absorption spectrophotometer for K. To carry out the elemental analysis measurements, the samples were dissolved in water by assistance of  $\text{H}_2\text{O}_2$  as these imidazole salts have poor solubility in water. Infrared spectra were recorded with an Alpha Centaur FTIR spectrometer in the 4000–400  $\text{cm}^{-1}$  region. X-ray powder diffraction (XRPD) patterns were recorded with a Siemens D5005 diffractometer with  $\text{Cu-K}\alpha$  ( $\lambda = 1.5418 \text{ \AA}$ ) radiation. Thermogravimetry was carried out with a Perkin–Elmer TGA-7 instrument in flowing  $\text{N}_2$  with a heating rate of  $10 \text{ }^\circ\text{C min}^{-1}$  up to  $800 \text{ }^\circ\text{C}$ . Electrochemical data were obtained with a CHI 660 Electrochemical Workstation connected to a Digital-586 personal computer under  $\text{N}_2$  gas, with the use of a conventional three-electrode system.

**Synthesis of  $(\text{HIm})_8\{\text{K}(\text{H}_2\text{O})\}_2\{(\mu_3\text{-H}_2\text{O})\text{Mn}(\text{H}_2\text{O})\}(\text{Si}_2\text{W}_{20}\text{O}_{70})\cdot 10\text{H}_2\text{O}(\text{Im} = \text{imidazole})$  (1):** Solid  $\text{MnSO}_4\cdot 2\text{H}_2\text{O}$  (0.076 g, 0.41 mmol) was added with stirring to a solution of imidazole (0.55 g, 2.3 mmol) dissolved in water (20 mL). Glacial acetic acid was then added dropwise until pH 3.6 was reached. To the resulting solution,  $K_8[\gamma\text{-SiW}_{10}\text{O}_{36}]\cdot 12\text{H}_2\text{O}$  (0.226 g, 0.075 mmol) dissolved in water (2 mL) was immediately added, followed by the addition of solid KCl (2–3 g, ca. 30 mmol). Finally, the yellow solution was cooled to room temperature and filtered through a fine frit. Prism-like yellow crystals were obtained after 3 d from the filtrate. Yield: 0.142 g (65% based on  $\gamma\text{-SiW}_{10}$ ). IR (KBr pellet): 1093, 1049, 993, 950, 894, 861, 781, 741, 621, 555  $\text{cm}^{-1}$ .  $\text{C}_{24}\text{H}_{35.76}\text{K}_2\text{MnN}_{16}\text{O}_{84}\cdot \text{Si}_2\text{W}_{20}$  (5758.57): calcd. W 63.22, Si 0.96, Mn 0.94, K, 1.34; found W 63.09, Si 0.92, Mn 0.96, K 1.30.

**Synthesis of  $(\text{HIm})_8\{\text{K}(\text{H}_2\text{O})\}_2\{(\mu_3\text{-H}_2\text{O})\text{Co}(\text{H}_2\text{O})\}(\text{Si}_2\text{W}_{20}\text{O}_{70})\cdot 9\text{H}_2\text{O}$  (2):** The synthesis of **2** followed a similar procedure to that of compound **1**, except  $\text{Co}(\text{NO}_3)_2\cdot 6\text{H}_2\text{O}$  (0.058 g, 0.20 mmol) was used instead of  $\text{MnSO}_4\cdot 2\text{H}_2\text{O}$ . The reaction solution was heated to  $45 \text{ }^\circ\text{C}$  with stirring for 15 min and filtered for lustration. Prism-like rosy crystals were obtained after ca. 6 d from the filtrate. Yield: 0.113 g (52% based on  $\gamma\text{-SiW}_{10}$ ). IR (KBr pellet): 1098, 1051, 998, 952, 897, 863, 778, 743, 622, 549  $\text{cm}^{-1}$ .  $\text{C}_{24}\text{H}_{31.5}\text{K}_2\text{CoN}_{16}\text{O}_{83}\cdot \text{Si}_2\text{W}_{20}$

(5742.26): calcd. W 63.92, Si 0.97, Co 1.02, K 1.36; found W 63.73, Si 0.94, Co 1.09, K 1.32.

**Synthesis of  $(\text{HIm})_8\{\text{K}(\text{H}_2\text{O})\}_2\{(\mu_3\text{-H}_2\text{O})\text{Ni}(\text{H}_2\text{O})\}(\text{Si}_2\text{W}_{20}\text{O}_{70})\cdot 9\text{H}_2\text{O}$  (3):** The synthesis of **3** followed a similar procedure to that of compound **2**, except  $\text{NiSO}_4\cdot 6\text{H}_2\text{O}$  (0.105 g, 0.40 mmol) was used instead of  $\text{Co}(\text{NO}_3)_2\cdot 6\text{H}_2\text{O}$ . Prism-like slight green crystals were obtained after six months. Yield: 0.022 g (10% based on  $\gamma\text{-SiW}_{10}$ ). IR (KBr pellet): 1091, 1049, 995, 951, 895, 861, 781, 739, 626, 554  $\text{cm}^{-1}$ .  $\text{C}_{24}\text{H}_{26}\text{K}_2\text{NiN}_{16}\text{O}_{83}\cdot \text{Si}_2\text{W}_{20}$  (5736.70): calcd. W 64.3, Si 0.97, Ni 1.03, K 1.36; found W 64.05, Si 0.92, Ni 0.98, K 1.29.

**X-ray Crystallography:** Single-crystals of **1** ( $0.37\times 0.11\times 0.10 \text{ mm}$ ), **2** ( $0.24\times 0.07\times 0.05 \text{ mm}$ ), and **3** ( $0.35\times 0.12\times 0.05 \text{ mm}$ ) were taken directly from the mother liquor and immediately cooled to 193(2) K on a Bruker SMART CCD diffractometer with graphite-monochromated  $\text{Mo-K}\alpha$  radiation ( $\lambda = 0.71073 \text{ \AA}$ ). Semi-empirical absorption correction based on symmetry equivalent reflections was applied. A total of 53450 reflections for **1** were collected, of which 9634 were unique ( $R_{\text{int}} = 0.0531$ ), a total of 52611 reflections for **2** were collected, of which 9454 reflections were unique ( $R_{\text{int}} = 0.0516$ ), and a total of 58285 reflections for **3** were collected, of which 10568 reflections were unique ( $R_{\text{int}} = 0.1003$ ) ( $1.52 < \theta < 25.01^\circ$ ). The structures were solved by direct methods and difference Fourier techniques and refined by the full-matrix least-squares method on the basis of  $F^2$ . Structure solution, refinement, and generation of publication materials were performed with the use of the SHELXTL crystallographic software package.<sup>[29]</sup> Some C and N atoms and some water molecules were not anisotropically refined to solve disorder. The hydrogen atoms of imidazole and water were geometrically placed and refined with the use of a riding model. However, some hydrogen atoms have not been included in the final refinement because of the presence of some disordered imidazole and water. Crystallographic data are summarized in Table 4. Atomic coordinates and isotropic displacement parameters for the anions of **1**, **2**, and **3** are listed in Tables S2, S3, and S4. CCDC-294280 for **1**, -294279 for **2**, and -604702 for **3** contain the supplementary crystallographic data for this paper. These data can be obtained free of charge from The Cambridge Crystallographic Data Centre via [www.ccdc.cam.ac.uk/data\\_request/cif](http://www.ccdc.cam.ac.uk/data_request/cif).

**Supporting Information** (see footnote on the first page of this article): Tables of atomic coordinates and isotropic displacement parameters, figures showing coordination spheres of  $\text{K}^+$  and  $\text{M}^{2+}$  for

Table 4. Crystal data and structure refinement for **1**, **2**, and **3**.

	<b>1</b>	<b>2</b>	<b>3</b>
Empirical formula	$\text{C}_{48}\text{H}_{71.52}\text{K}_4\text{Mn}_2\text{N}_{32}\text{O}_{168}\text{Si}_4\text{W}_{40}$	$\text{C}_{48}\text{H}_{63}\text{Co}_2\text{K}_4\text{N}_{32}\text{O}_{166}\text{Si}_4\text{W}_{40}$	$\text{C}_{48}\text{H}_{52}\text{K}_4\text{N}_{32}\text{Ni}_2\text{O}_{166}\text{Si}_4\text{W}_{40}$
Formula mass	11517.13	11484.52	11444.93
Space group	<i>Pnma</i>	<i>Pnma</i>	<i>Pnma</i>
<i>a</i> [ $\text{\AA}$ ]	33.1566(14)	32.9856(15)	32.947(2)
<i>b</i> [ $\text{\AA}$ ]	13.6167(6)	13.5564(6)	13.5430(10)
<i>c</i> [ $\text{\AA}$ ]	22.9345(10)	22.9521(11)	22.9577(16)
<i>V</i> [ $\text{\AA}^3$ ]	10354.5(8)	10263.4(8)	10243.8(12)
<i>Z</i>	2	2	2
<i>D</i> <sub>calcd.</sub> [ $\text{g cm}^{-3}$ ]	3.694	3.716	3.711
<i>T</i> [K]	193(2)	193(2)	193(2)
$\lambda$ [ $\text{\AA}$ ]	0.71073	0.71073	0.71073
$\mu$ [ $\text{mm}^{-1}$ ]	22.447	22.684	22.748
GOF	1.058	1.059	1.026
Final $R_1$ <sup>[a]</sup> [ $I > 2\sigma(I)$ ]	0.0529	0.0483	0.0564
Final $wR_2$ <sup>[b]</sup> [ $I > 2\sigma(I)$ ]	0.1478	0.1350	0.1689

[a]  $R_1 = \Sigma||F_o| - |F_c||/|F_o|$ . [b]  $wR_2 = \{\Sigma[w(F_o^2 - F_c^2)^2]/\Sigma[w(F_o^2)^2]\}^{0.5}$ .

compounds **2** and **3**, XRD, IR, TG, and X-ray crystallographic data of compounds **1**, **2** and **3**.

## Acknowledgments

This work was supported by the National Natural Science Foundation of China (No. 20671016).

- [1] a) M. T. Pope, *Heteropoly and Isopoly Oxometalates*, Springer, Berlin, **1983**; b) P. Kögerler, L. Cronin, *Angew. Chem. Int. Ed.* **2005**, *44*, 844–846.
- [2] a) M. T. Pope, A. Müller, *Angew. Chem. Int. Ed. Engl.* **1991**, *30*, 34–48; b) Y. Nakagawa, K. Uehara, N. Mizuno, *Inorg. Chem.* **2005**, *44*, 14–16; c) T. Hayashi, A. Kishida, N. Mizuno, *Chem. Commun.* **2000**, 381–382; d) K. Kamata, K. Yonehara, Y. Sumida, K. Yamaguchi, S. Hikichi, N. Mizuno, *Science* **2003**, *300*, 964–966; e) Y. Nishiyama, Y. Nakagawa, N. Mizuno, *Angew. Chem. Int. Ed.* **2001**, *40*, 3639–3641.
- [3] a) S. Bareyt, S. Piligkos, B. Hasenknopf, P. Gouzerh, E. Lacote, S. Thorimbert, M. Malacria, *J. Am. Chem. Soc.* **2005**, *127*, 6788–6794; b) L. H. Bi, U. Kortz, *Inorg. Chem.* **2004**, *43*, 7961–7962.
- [4] J. Canny, A. Tézé, R. Thouvenot, G. Hervé, *Inorg. Chem.* **1986**, *25*, 2114–2119.
- [5] X.-Y. Zhang, C. J. O'Connor, G. B. Jameson, M. T. Pope, *Inorg. Chem.* **1996**, *35*, 30–34.
- [6] K. Wassermann, H. J. Lunk, R. Palm, J. Fuchs, N. Steinfeldt, R. Stösser, M. T. Pope, *Inorg. Chem.* **1996**, *35*, 3273–3279.
- [7] C. Nozaki, I. Kiyoto, Y. Minai, M. Misono, N. Mizuno, *Inorg. Chem.* **1999**, *38*, 5724–5729.
- [8] J. Canny, R. Thouvenot, A. Tézé, G. Hervé, M. Leparulo-Loftus, M. T. Pope, *Inorg. Chem.* **1991**, *30*, 976–981.
- [9] C. R. Mayer, I. Fournier, R. Thouvenot, *Chem. Eur. J.* **2000**, *6*, 105–110.
- [10] E. Cadot, V. Béreau, B. Marg, S. Halut, F. Sécheresse, *Inorg. Chem.* **1996**, *35*, 3099–3106.
- [11] C. R. Mayer, P. Herson, R. Thouvenot, *Inorg. Chem.* **1999**, *38*, 6152–6158.
- [12] B. Botar, Y. V. Geletii, P. Kogerler, D. G. Musaev, K. Morokuma, I. A. Weinstock, C. L. Hill, *Dalton Trans.* **2005**, 2017–2021.
- [13] a) F. Xin, M. T. Pope, *Inorg. Chem.* **1996**, *35*, 5693–5695; b) F. Xin, M. T. Pope, G. J. Long, U. Russo, *Inorg. Chem.* **1996**, *35*, 1207–1213; c) During the preparation of this paper, three potassium salts of decatungstosilicate dimers were reported: B. S. Bassil, M. H. Dickman, M. Reicke, U. Kortz, B. Keitab, L. Nadjo, *Dalton Trans.* **2006**, 4253. DOI: 10.1039/b606911h.
- [14] U. Kortz, S. Isber, M. H. Dickman, D. Ravot, *Inorg. Chem.* **2000**, *39*, 2915–2922.
- [15] U. Kortz, Y. P. Jeannin, A. Tézé, G. Hervé, S. Isber, *Inorg. Chem.* **1999**, *38*, 3670–3675.
- [16] F. Hussain, B. S. Bassil, L. H. Bi, M. Reicke, U. Kortz, *Angew. Chem. Int. Ed.* **2004**, *43*, 3485–3488.
- [17] B. S. Bassil, S. Nellutla, U. Kortz, A. C. Stowe, J. van Tol, N. S. Dalal, B. Keita, L. Nadjo, *Inorg. Chem.* **2005**, *44*, 2659–2665.
- [18] U. Kortz, S. Matta, *Inorg. Chem.* **2001**, *40*, 815–817.
- [19] B. S. Bassil, U. Kortz, A. S. Tigan, J. M. Clemente-Juan, B. Keita, P. de Oliveira, L. Nadjo, *Inorg. Chem.* **2005**, *44*, 9360–9368.
- [20] A. Tézé, M. Michelin, G. Hervé, *Inorg. Chem.* **1997**, *36*, 5666–5669.
- [21] a) J. Peng, W. Z. Li, E. B. Wang, Q. L. Bai, *J. Chem. Soc., Dalton Trans.* **2001**, 3668–3671; b) J. Peng, H. Y. Ma, Z. G. Han, B. X. Dong, W. Z. Li, J. Lu, E. B. Wang, *Dalton Trans.* **2003**, 3850–3855.
- [22] N. Leclerc-Laronze, J. Marrot, G. Hervé, *Inorg. Chem.* **2005**, *44*, 1275–1281.
- [23] D. G. Musaev, K. Morokuma, Y. V. Geletii, C. L. Hill, *Inorg. Chem.* **2004**, *43*, 7702–7708.
- [24] I. D. Brown, D. Altermatt, *Acta Crystallogr., Sect. B* **1985**, *41*, 244–247.
- [25] A. Tézé, J. Canny, L. Gurban, R. Thouvenot, G. Hervé, *Inorg. Chem.* **1996**, *35*, 1001–1005.
- [26] N. Leclerc-Laronze, J. Marrot, G. Hervé, *Inorg. Chem.* **2003**, *42*, 5857–5862.
- [27] T. M. Anderson, W. A. Neiwert, C. L. Hill, *Inorg. Chem.* **2004**, *43*, 7353–7358.
- [28] A. Tézé, G. Hervé, *Inorg. Synth.* **1990**, *27*, 85–88.
- [29] G. M. Sheldrick, *SHELXS-97, Program for Crystal Structure Solution*, University of Göttingen, Germany, **1997**.

Received: August 1, 2006

Published Online: October 12, 2006